STRUCTURAL CHEMISTRY
ISSN 2053-2296

Crystal structure and spectroscopic characterization of a cobalt(II) tetraazamacrocycle: completing a series of first-row transition-metal complexes

Katherine M. Van Heuvelen,[a]* Isabell Lee,[a] Katherine Arriola,[a] Rilke Griffin,[a] Christopher Ye[a] and Michael K. Takase[b]

[a]Department of Chemistry, Harvey Mudd College, 301 Platt Blvd, Claremont, CA 91711, USA, and [b]Beckman Institute, California Institute of Technology, 1200 E. California Blvd, Pasadena, CA 91125, USA. *Correspondence e-mail: vanheuvelen@g.hmc.edu

Received 29 April 2017
Accepted 13 July 2017

Edited by G. P. A. Yap, University of Delaware, USA

Keywords: divalent cobalt; tetraazamacrocycle; UV–visible spectroscopy; density functional theory; crystal structure; computational chemistry.

CCDC reference: 1562037

Supporting information: this article has supporting information at journals.iucr.org/c

The tetraazamacrocyclic ligand 1,4,8,11-tetramethyl-1,4,8,11-tetraazacyclotetradecane (TMC) has been used to bind a variety of first-row transition metals but to date the crystal structure of the cobalt(II) complex has been missing from this series. The missing cobalt complex chlorido(1,4,8,11-tetramethyl-1,4,8,11-tetraazacyclotetradecane-κ^4N)cobalt(II) chloride dihydrate, $[CoCl(C_{14}H_{32}N_4)]Cl{\cdot}2H_2O$ or $[Co^{II}Cl(TMC)]Cl{\cdot}2H_2O$, crystallizes as a purple crystal. This species adopts a distorted square-pyramidal geometry in which the TMC ligand assumes the *trans*-I configuration and the chloride ion binds in the *syn*-methyl pocket of the ligand. The Co^{II} ion adopts an $S = \frac{3}{2}$ spin state, as measured by the Evans NMR method, and UV–visible spectroscopic studies indicate that the title hydrated salt is stable in solution. Density functional theory (DFT) studies reveal that the geometric parameters of $[Co^{II}Cl(TMC)]Cl{\cdot}2H_2O$ are sensitive to the cobalt spin state and correctly predict a change in spin state upon a minor perturbation to the ligand environment.

1. Introduction

Since its first report by Barefield & Wagner (1973), the tetraazamacrocyclic ligand 1,4,8,11-tetramethyl-1,4,8,11-tetraazacyclotetradecane (TMC) has been used to bind a variety of first-row transition metals. A search of the Cambridge Structural Database (CSD; Groom *et al.*, 2016) showed crystal structures of *M*(TMC) complexes, where *M* ranges from chromium to zinc. In addition to its versatility in binding first-row transition-metal ions, TMC also provides a scaffold for accessing a wide range of isomers. On complexation, the TMC ligand commonly adopts the *trans* configuration, with a roughly square-planar geometry, in which the four N atoms occupy the equatorial plane and there are two axial binding sites for exogenous ligands. There are five possible diastereomers of the *trans* configuration, two of which are shown in Fig. 1. The *trans*-I isomer contains two binding pockets that can be distinguished as *syn*-methyl and *anti*-methyl. An isomer with two *cis*-binding sites may be accessed as well (Barefield,

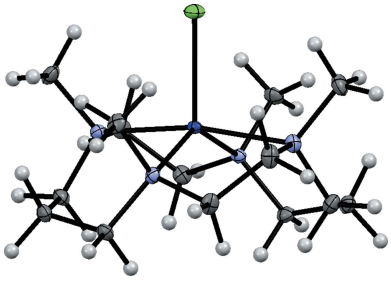

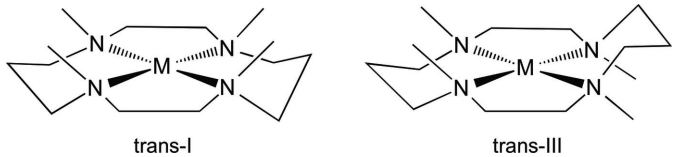

Figure 1
Select *trans* isomers of the TMC ligand (adapted from Barefield, 2010).

2010). Divalent metal salts of TMC also serve as versatile starting materials for preparing a wide range of reactive complexes, for example, metal–oxygen adducts (Cho *et al.*, 2010; Kieber-Emmons & Riordan, 2007), and for accessing high-valent metal oxidation states (Rohde *et al.*, 2003; Van Heuvelen *et al.*, 2012). First-row transition-metal complexes of the form $[M^{II}Cl(TMC)]^+$ [*M* = Mn (Bucher *et al.*, 2001), Fe (Bedford *et al.*, 2016), Ni (Nishigaki *et al.*, 2010), and Zn (Alcock *et al.*, 1978)] have been crystallographically characterized and reported in the CSD, but to date the crystal structure of $[Co^{II}Cl(TMC)]^+$ has been missing from this series. In this work, we describe the synthesis, crystallization, and characterization of $[Co^{II}Cl(TMC)]Cl{\cdot}2H_2O$, (1).

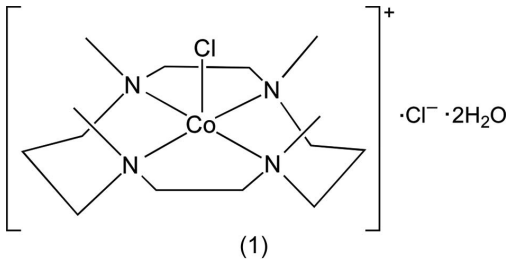

(1)

2. Experimental

2.1. Synthesis and crystallization

Starting materials were obtained from Sigma–Aldrich. $CoCl_2{\cdot}6H_2O$ (0.2704 g, 1.14 mmol) and 1,4,8,11-tetramethyl-1,4,8,11-tetraazacyclotetradecane (0.2967 g, 1.16 mmol) were combined under a nitrogen atmosphere, dissolved in acetonitrile (20 ml), and heated under reflux for 22 h to yield a violet solution. The solvent was removed under reduced pressure, and the product was recrystallized by vapor diffusion (acetonitrile/diethyl ether) at 277 K to yield purple crystals (yield 79%). Elemental analysis data were obtained from Atlantic Microlabs. Analysis calculated for $C_{14}H_{36}Cl_2CoN_4O_2$: C 39.81, H 8.59, N 13.27%; found: C 39.92, H 8.49, N 12.93%. λ_{max} (ε, nm) in acetonitrile: 510 (37 M^{-1} cm^{-1}), 560 (23 M^{-1} cm^{-1}), 810 (13 M^{-1} cm^{-1}), 931 (15 M^{-1} cm^{-1}).

2.2. Refinement

Crystal data, data collection and structure refinement details are summarized in Table 1. Unless otherwise noted, all H atoms were included in the model at geometrically calculated positions and refined using a riding model. The isotropic displacement parameters of all H atoms were fixed at 1.2 times the U_{eq} value of the atoms to which they are linked (1.5 times for methyl groups and water). Complex (1) crystallizes in the monoclinic space group $P2_1/c$ with one cation in the asymmetric unit, together with one chloride anion and two water molecules. The coordinates for the H atoms bound to atoms O1*W* and O2*W* were located in the difference Fourier synthesis and refined semi-freely with the help of a restraint on the O—H distance [0.84 (2) Å].

Table 1
Experimental details.

Crystal data	
Chemical formula	$[CoCl(C_{14}H_{32}N_4)]Cl{\cdot}2H_2O$
M_r	422.30
Crystal system, space group	Monoclinic, $P2_1/c$
Temperature (K)	100
a, *b*, *c* (Å)	8.2864 (8), 17.0679 (16), 13.9733 (14)
β (°)	90.735 (4)
V (Å^3)	1976.1 (3)
Z	4
Radiation type	Mo $K\alpha$
μ (mm^{-1})	1.15
Crystal size (mm)	0.40 × 0.30 × 0.25
Data collection	
Diffractometer	Bruker D8 VENTURE Kappa Duo PHOTON 100 CMOS
Absorption correction	Multi-scan (*SADABS*; Bruker, 2013)
T_{min}, T_{max}	0.691, 0.747
No. of measured, independent and observed [$I > 2\sigma(I)$] reflections	72258, 9577, 7769
R_{int}	0.043
$(\sin\theta/\lambda)_{max}$ (Å^{-1})	0.834
Refinement	
$R[F^2 > 2\sigma(F^2)]$, $wR(F^2)$, S	0.032, 0.066, 1.04
No. of reflections	9577
No. of parameters	224
No. of restraints	4
H-atom treatment	H atoms treated by a mixture of independent and constrained refinement
$\Delta\rho_{max}$, $\Delta\rho_{min}$ (e Å^{-3})	0.56, −0.56

Computer programs: *APEX3* (Bruker, 2017), *SAINT* (Bruker, 2013), *SHELXS2013* (Sheldrick, 2008), *SHELXL2016* (Sheldrick, 2015) and *SHELXTL* (Sheldrick, 2008).

2.3. Spectroscopy and computations

UV–visible spectra were collected on an Agilent 8453 diode array spectrometer equipped with a Hewlett Packard 89090A temperature-control unit, and these studies considered acetonitrile, methanol, and chloroform as solvents. The Evans NMR method (Evans, 1959; Evans *et al.*, 1971; Evans & Jakubovic, 1988; Sur, 1989) was used to measure magnetic susceptibility at 298 K. Data were collected using a Bruker 400 MHz spectrometer and considered samples ranging from 0.0064 to 0.0076 *M* prepared in $CDCl_3$. Corrections for the diamagnetic susceptibility of the cobalt ion, chloride, and TMC ligand were applied (Bain & Berry, 2008). Density functional theory (DFT) geometry optimizations and frequency calculations were implemented on the Extreme Scientific and Engineering Discovery Environment (XSEDE) (Towns *et al.*, 2014) using the *GAUSSIAN09* software package (Frisch *et al.*, 2013). The keyword 'scf=tight' specified the convergence criteria. We evaluated several functionals (B3LYP, BP86, M06, and PBEPBE) and basis sets [def2TZVPP/def2svp, 6-311G(d)/6-31G(d), and 6-31G/3-21G, as applied to cobalt/all other atoms]. The unrestricted functional M06 (Zhao & Truhlar, 2008), along with the 6-31G basis set (Petersson & Al-Laham, 1991; Petersson *et al.*, 1988), on Co and the 3-21G basis set (Binkley *et al.*, 1980) on all other

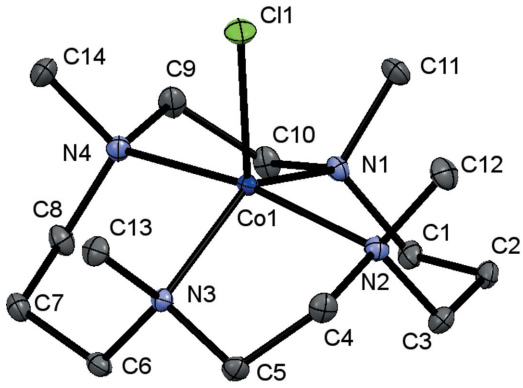

Figure 2
The cation of $[Co^{II}Cl(TMC)]Cl{\cdot}2H_2O$, (1), showing the atom-numbering scheme. Displacement ellipsoids are drawn at the 50% probability level. H atoms have been omitted for clarity.

atoms best reproduced the experimentally observed bond lengths and were used for the results reported herein.

3. Results and discussion

X-ray diffraction studies of the purple crystals showed that complex (1) crystallized in the monoclinic $P2_1/c$ space group. Selected geometric parameters are reported in Table 2. The Co—N bond lengths found in complex (1) are consistent with previous reports of analogous five-coordinate $[Co^{II}(TMC)X]^{n+}$ cations [X = NCS^- (Burgess *et al.*, 1999), N_3^- (Evangelio *et al.*, 2012; Reimer *et al.*, 1989), and CH_3CN (Jo *et al.*, 2008)]. The Co—Cl bond length of 2.3022 (3) Å falls within the range of M—Cl bond lengths observed for zinc [2.265 (4) Å], nickel [2.3074 (17) Å], and manganese [2.331 (1) Å] complexes of the form $[MCl(TMC)]^+$ (Alcock *et al.*, 1978; Bucher *et al.*, 2001; Nishigaki *et al.*, 2010). The analogous iron complex contains an unusually short Fe^{II}—Cl bond length of 2.2051 Å (Bedford *et al.*, 2016). The second chloride ion in the structure of complex (1) does not coordinate to cobalt and instead lies approximately 5 Å away from the metal center. Complex (1) adopts a distorted square-pyramidal geometry (τ = 0.53, where a τ value of 0.00 is associated with a square-pyramidal geometry and a τ value of 1.00 is associated with an ideal trigonal bipyramidal geometry; Addison *et al.*, 1984).

Table 2
Selected geometric parameters (Å, °).

Cl1—Co1	2.3022 (3)	Co1—N2	2.2208 (9)
Co1—N3	2.1066 (8)	Co1—N4	2.2427 (9)
Co1—N1	2.1158 (8)		
N3—Co1—N1	137.57 (3)	N2—Co1—N4	169.13 (3)
N3—Co1—N2	84.26 (3)	N3—Co1—Cl1	112.70 (2)
N1—Co1—N2	92.53 (3)	N1—Co1—Cl1	109.71 (2)
N3—Co1—N4	91.52 (3)	N2—Co1—Cl1	96.12 (2)
N1—Co1—N4	83.81 (3)	N4—Co1—Cl1	94.75 (2)

Table 3
Hydrogen-bond geometry (Å, °).

D—H···A	D—H	H···A	D···A	D—H···A
C2—H2A···Cl2^{i}	0.99	2.83	3.7784 (11)	160
C3—H3A···Cl2^{ii}	0.99	2.74	3.7054 (11)	166
C11—H11C···O1W^{i}	0.98	2.66	3.5203 (13)	147
C5—H5A···Cl2^{ii}	0.99	2.76	3.7452 (10)	171
C12—H12A···Cl1	0.98	2.77	3.3409 (11)	118
C7—H7A···Cl2^{iii}	0.99	2.94	3.6790 (10)	132
C8—H8A···O2W^{ii}	0.99	2.66	3.6324 (14)	168
C13—H13C···Cl2^{iv}	0.98	2.97	3.7640 (10)	138
C9—H9B···O1W^{v}	0.99	2.58	3.4736 (13)	150
C10—H10A···O2W^{ii}	0.99	2.54	3.5121 (14)	168
C14—H14A···Cl1	0.98	2.70	3.3189 (12)	122
O2W—H2W2···Cl2^{vi}	0.82 (1)	2.40 (1)	3.2158 (9)	173 (2)
O2W—H2W1···Cl2	0.83 (1)	2.39 (1)	3.2110 (9)	175 (2)
O1W—H1W1···Cl1	0.87 (1)	2.39 (1)	3.2568 (9)	173 (1)
O1W—H1W2···Cl2	0.87 (1)	2.33 (1)	3.2024 (9)	178 (1)

Symmetry codes: (i) $x+1, y, z$; (ii) $x+1, -y+\frac{3}{2}, z+\frac{1}{2}$; (iii) $-x+1, y-\frac{1}{2}, -z+\frac{3}{2}$; (iv) $x, -y+\frac{3}{2}, z+\frac{1}{2}$; (v) $-x+1, -y+1, -z+1$; (vi) $-x, -y+2, -z+1$.

The TMC ligand in complex (1) adopts the *trans*-I configuration (Fig. 1), in which all four methyl groups are positioned on the same side of the plane, as is typical for divalent transition metal complexes of TMC (Barefield, 2010). The chloride ligand occupies the *syn*-methyl binding site (Fig. 2). This is consistent with studies of similar $[Co^{II}(TMC)X]^{n+}$ complexes [X = NCS^- (Burgess *et al.*, 1999), N_3^- (Evangelio *et al.*, 2012; Reimer *et al.*, 1989), and CH_3CN (Jo *et al.*, 2008)], as well as $[M^{II}Cl(TMC)]^+$ [M = Mn, Fe, Ni; Bedford *et al.*, 2016; Bucher *et al.*, 2001; Nishigaki *et al.*, 2010].

Two chloride anions and two water molecules form a hydrogen-bonded dimer across a crystallographic inversion

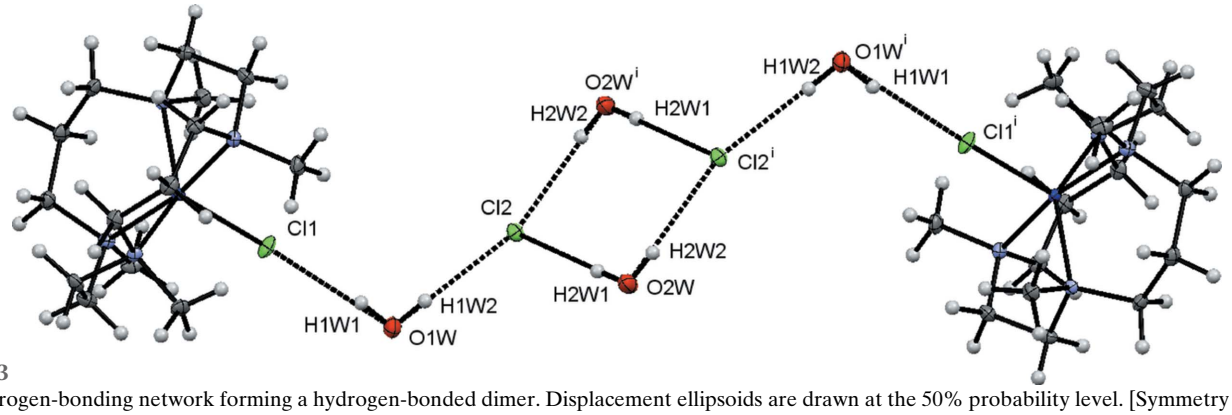

Figure 3
The hydrogen-bonding network forming a hydrogen-bonded dimer. Displacement ellipsoids are drawn at the 50% probability level. [Symmetry code: (i) $-x, -y+2, -z+1$.]

Table 4
Comparison of experimental and calculated (DFT) geometric parameters (Å) of complex (1).

	Experimental	DFT
Cl1—Co1	2.3022 (3)	2.3163
Co1—N3	2.1066 (8)	2.1008
Co1—N1	2.1158 (8)	2.1008
Co1—N2	2.2208 (9)	2.1980
Co1—N4	2.2427 (9)	2.1981

center (Fig. 3 and Table 3). The core of the dimer consists of two water molecules [O2*W* and O2*W*^{i}; symmetry code: (i) $-x$, $-y+2$, $-z+1$] and two chloride anions (Cl2 and Cl2^{i}). On each side of this core, the hydrogen bonding extends to a water molecule (O1*W* and O1*W*^{i}) and the chloride anion in the cobalt chloride complex (Cl1 and Cl1^{i}).

Fig. 4 shows the electronic absorption spectrum of complex (1) in acetonitrile with optical features apparent at 510 (37 M^{-1} cm^{-1}), 560 (23 M^{-1} cm^{-1}), 810 (13 M^{-1} cm^{-1}), and 931 nm (15 M^{-1} cm^{-1}). The magnitude of the molar absorptivity values range from 13 to 37 M^{-1} cm^{-1}, which suggests these features arise from *d*-to-*d* ligand field transitions.

Acetonitrile is known to coordinate to transition-metal cations ligated by TMC (Jo *et al.*, 2008; Rohde *et al.*, 2003). We compared the spectral features of complex (1) to those reported for $[Co(TMC)(CH_3CN)]^{2+}$ to determine if acetonitrile displaces the chloride ligand in solution, as UV–visible spectroscopy is sensitive to changes in the axial ligand (Jackson *et al.*, 2008; Jo *et al.*, 2008). The UV–visible spectrum of the acetonitrile-bound complex exhibited absorption features at 447 (50 M^{-1} cm^{-1}), 532 (35 M^{-1} cm^{-1}), 547 (35 M^{-1} cm^{-1}), 643 (17 M^{-1} cm^{-1}), and 667 nm (18 M^{-1} cm^{-1}) (Jo *et al.*, 2008). The differences between the spectra obtained for complex (1) and for $[Co(TMC)(CH_3CN)]^{2+}$ indicate that acetonitrile does not coordinate to complex (1) in solution. UV–visible spectra collected in the absence of acetonitrile confirm this result. A sample of complex (1) prepared in methanol showed essentially identical spectral features as were obtained in acetonitrile (see Fig. S2 in the supporting information). Similar results were obtained for a sample of complex (1) prepared in the noncoordinating solvent chloroform, which was also used as a solvent in the NMR experiments used to determine μ_{eff} (see below). As with the methanol sample, only the minor spectral changes that are typically associated with changes in solvent systems were observed in the sample prepared with chloroform (see Fig. S2 in the supporting information). Finally, UV–visible spectroscopic studies demonstrate that complex (1) is stable in solution for several hours at room temperature; spectra of samples prepared in acetonitrile and in chloroform showed no change in the intensity or the position of spectral features over several hours (see Figs. S3 and S4 in the supporting information).

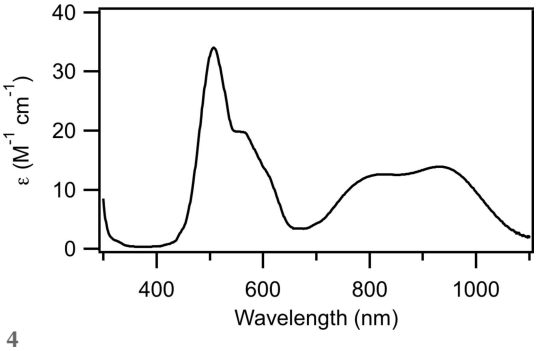

Figure 4
UV–visible absorption spectrum of complex (1) in acetonitrile.

Barefield reports that divalent $[M(TMC)]^{2+}$ (M = Mn, Fe, Co, Ni) complexes are high-spin (Barefield, 2010), but recent results in the literature indicate that minor perturbations to the ligand ring size can affect the cobalt spin state. The 14-membered TMC ligand differs from 13-TMC by a single C atom (13-TMC is 1,4,7,10-tetramethyl-1,4,7,10-tetraazacyclotridecane). Electron paramagnetic resonance (EPR) studies of $[Co(13\text{-}TMC)(CH_3CN)]^{2+}$ conducted at 4.3 K revealed an $S=\frac{1}{2}$ spin state. This low spin state was also reported for $[Co(12\text{-}TMC)(CH_3CN)]^{2+}$ (12-TMC is 1,4,7,10-tetramethyl-1,4,7,10-tetraazacyclododecane) (Cho *et al.*, 2010). In contrast, EPR studies at 4.3 K demonstrate that $[Co(TMC)(CH_3CN)]^{2+}$ is in the $S=\frac{3}{2}$ spin state typical for divalent $[M(TMC)]^{2+}$ complexes (Jo *et al.*, 2008). The average Co—N bond lengths of 1.988 and 2.068 Å observed in $[Co^{II}(12\text{-}TMC)(MeCN)]^{2+}$ and $[Co^{II}(13\text{-}TMC)(MeCN)]^{2+}$, respectively, are shorter than those observed for complex (1), and crystal field theory indicates that a contraction of metal–ligand bond lengths is consistent with a change in spin state.

Since spin state is an important parameter in transition-metal chemistry, we probed the spin state of complex (1) using experimental and computational methods. NMR studies using the Evans method (Evans, 1959) were conducted to conclusively determine the cobalt ion spin state in complex (1). The experimental value of μ_{eff} = 4.56±0.06 Bohr magnetons (μ_B) is larger than expected for an $S=\frac{3}{2}$ complex. However, this value is consistent with the significant spin-orbit coupling observed in high-spin Co^{II} complexes, and the measured value of 4.56±0.06 μ_B falls within the range of experimental μ_{eff} values of 4.1 to 5.2 μ_B reported by Drago for high-spin Co^{II} complexes (Drago, 1992; Shaffer *et al.*, 2016).

The spin state of complex (1) was also investigated using density functional theory (DFT), as implemented in the *GAUSSIAN09* software package (Frisch *et al.*, 2013). Geometry optimization and frequency calculations considered two possible spin states, *viz.* $S=\frac{3}{2}$ and a hypothetical $S=\frac{1}{2}$ state. We evaluated the performance of a variety of unrestricted functionals (B3LYP, BP86, M06, and PBEPBE) and basis sets [def2TZVPP/def2svp, 6-311G(d)/6-31G(d), and 6-31G/3-21G, as applied to cobalt/all other atoms]. The hybrid functional M06, which was parameterized for transition-metal systems (Zhao & Truhlar, 2008; Cramer & Truhlar, 2009), along with the 6-31G basis set on Co and the 3-21G basis set on all other atoms, best reproduced the experimentally observed bond lengths (Table 4). As expected from crystal field theory and in agreement with experimental studies of $[Co^{II}(12\text{-}TMC)(MeCN)]^{2+}$ and $[Co^{II}(13\text{-}TMC)(MeCN)]^{2+}$, the Co—N bonds of a hypothetical $S=\frac{1}{2}$ complex (1) contracted to 2.04 Å.

The $S = \frac{3}{2}$ state of complex (1) was calculated to be more stable than the $S = \frac{1}{2}$ state by 11.4 kcal mol^{-1}, and all combinations of basis sets and functionals properly reproduced the experimentally-observed spin state (see Table S4 in the supporting information).

To determine if this methodology correctly predicts the change in spin state upon a minor modification of the ligand environment, parallel DFT investigations considered the relative energies of the $S = \frac{3}{2}$ and $S = \frac{1}{2}$ spin states of $[Co^{II}(13\text{-}TMC)(MeCN)]^{2+}$. These studies employed the computational parameters validated through studies of complex (1) and used the reported crystal structure of $[Co^{II}(13\text{-}TMC)(MeCN)]^{2+}$ as an input geometry (Cho *et al.*, 2010). DFT studies correctly predict that the high spin $S = \frac{3}{2}$ state is *destabilized* relative to the low spin $S = \frac{1}{2}$ state (+2.7 kcal mol^{-1}) when a single C atom is removed from the ligand. In the case of TMC and 13-TMC, a minor perturbation to the ligand structure results in a significant change in the cobalt spin state.

4. Conclusions

In this paper, we report the structural and spectral properties of $[Co^{II}Cl(TMC)]Cl{\cdot}2H_2O$, which continues the series of first-row transition-metal complexes bound by the tetraaza-macrocyclic TMC ligand and an axial chloride ion. Complex (1) adopts a distorted square-pyramidal geometry, and the chloride ligand binds in the *syn*-methyl pocket of the TMC ligand. UV–visible spectroscopic studies demonstrate that the structure of complex (1) is stable in a variety of solvents. Experimental and computational studies confirm that the cobalt ion is in the $S = \frac{3}{2}$ state, and the experimentally-validated computational methodology correctly predicts the change in spin state upon minor perturbations to the ligand environment. This result demonstrates that the TMC ligand family offers a facile means of accessing different cobalt spin states.

Acknowledgements

We thank Professor Adam Johnson (Harvey Mudd College) for helpful discussions.

Funding information

This work was funded by the Department of Chemistry at Harvey Mudd College, the Hixon Center for Sustainable Environmental Design at Harvey Mudd College through its Rasmussen Summer Research Fund (to CY), the Rose Hills Foundation (to IL), and the Harris Family Research Fellowship in Chemistry honoring Professor Emeritus Philip C. Myhre (to RG). This work used the Extreme Science and Engineering Discovery Environment (XSEDE), which is supported by National Science Foundation grant No. ACI-1548562.

References

Addison, A. W., Rao, T. N., Reedijk, J., van Rijn, J. & Verschoor, G. C. (1984). *J. Chem. Soc. Dalton Trans.* pp. 1349–1356.
Alcock, N. W., Herron, N. & Moore, P. (1978). *J. Chem. Soc. Dalton Trans.* pp. 1282–1288.
Bain, G. A. & Berry, J. F. (2008). *J. Chem. Educ.* **85**, 532–536.
Barefield, E. K. (2010). *Coord. Chem. Rev.* **254**, 1607–1627.
Barefield, E. K. & Wagner, F. (1973). *Inorg. Chem.* **12**, 2435–2439.
Bedford, R. B., Brenner, P. B., Elorriaga, D., Harvey, J. N. & Nunn, J. (2016). *Dalton Trans.* **45**, 15811–15817.
Binkley, J. S., Pople, J. A. & Hehre, W. J. (1980). *J. Am. Chem. Soc.* **102**, 939–947.
Bruker (2013). *SAINT* and *SADABS*. Bruker AXS Inc., Madison, Wisconsin, USA.
Bruker (2017). *APEX3*. Bruker AXS Inc., Madison, Wisconsin, USA.
Bucher, C., Duval, E., Barbe, J. M., Verpeaux, J. N., Amatore, C., Guilard, R., Pape, L. L., Latour, J.-M., Dahaoui, S. & Lecomte, C. (2001). *Inorg. Chem.* **40**, 5722–5726.
Burgess, J., Fawcett, J., Haines, R. I., Singh, K. & Russell, D. R. (1999). *Transition Met. Chem.* **24**, 355–361.
Cho, J., Sarangi, R., Kang, H. Y., Lee, J. Y., Kubo, M., Ogura, T., Solomon, E. I. & Nam, W. (2010). *J. Am. Chem. Soc.* **132**, 16977–16986.
Cramer, C. J. & Truhlar, D. G. (2009). *Phys. Chem. Chem. Phys.* **11**, 10757–10816.
Drago, R. S. (1992). In *Physical Methods for Chemists*, 2nd ed. Fort Worth: Saunders College Publishing.
Evangelio, E., Rath, N. P. & Mirica, L. M. (2012). *Dalton Trans.* **41**, 8010–8021.
Evans, D. F. (1959). *J. Chem. Soc.* **36**, 2003–2005.
Evans, D. F., Fazakerley, G. V. & Phillips, R. F. (1971). *J. Chem. Soc. A*, pp. 1931–1934.
Evans, D. F. & Jakubovic, D. A. (1988). *J. Chem. Soc. Dalton Trans.* pp. 2927–2933.
Frisch, M. J., *et al.* (2013). *GAUSSIAN09*. Gaussian Inc., Wallingford, CT, USA. http://www.gaussian.com.
Groom, C. R., Bruno, I. J., Lightfoot, M. P. & Ward, S. C. (2016). *Acta Cryst.* B**72**, 171–179.
Jackson, T. A., Rohde, J. U., Seo, M. S., Sastri, C. V., DeHont, R., Stubna, A., Ohta, T., Kitagawa, T., Münck, E., Nam, W. & Que, L. (2008). *J. Am. Chem. Soc.* **130**, 12394–12407.
Jo, Y., Annaraj, J., Seo, M. S., Lee, Y.-M., Kim, S. Y., Cho, J. & Nam, W. (2008). *J. Inorg. Biochem.* **102**, 2155–2159.
Kieber-Emmons, M. T. & Riordan, C. G. (2007). *Acc. Chem. Res.* **40**, 618–625.
Nishigaki, J.-I., Matsumoto, T. & Tatsumi, K. (2010). *Eur. J. Inorg. Chem.* pp. 5011–5017.
Petersson, G. A. & Al-Laham, M. A. (1991). *J. Chem. Phys.* **94**, 6081–6090.
Petersson, G. A., Bennett, A., Tensfeldt, T. G., Al-Laham, M. A., Shirley, W. A. & Mantzaris, J. (1988). *J. Chem. Phys.* **89**, 2193–2218.
Reimer, S., Wicholas, M., Scott, B. & Willett, R. D. (1989). *Acta Cryst.* C**45**, 1694–1697.
Rohde, J. U., In, J.-H., Lim, M. H., Brennessel, W. W., Bukowski, M. R., Stubna, A., Munck, E., Nam, W. & Que, L. (2003). *Science*, **299**, 1037–1039.
Shaffer, D. W., Bhowmick, I., Rheingold, A. L., Tsay, C., Livesay, B. N., Shores, M. P. & Yang, J. Y. (2016). *Dalton Trans.* **45**, 17910–17917.
Sheldrick, G. M. (2008). *Acta Cryst.* A**64**, 112–122.
Sheldrick, G. M. (2015). *Acta Cryst.* C**71**, 3–8.
Sur, S. K. (1989). *J. Magnet. Reson.* **82**, 169–173.
Towns, J., Cockerill, T., Dahan, M., Foster, I., Gaither, K., Grimshaw, A., Hazlewood, V., Lathrop, S., Lifka, D., Peterson, G. D., Roskies, R., Scott, J. R. & Wilkins-Diehr, N. (2014). *Comput. Sci. Eng.* **16**, 62–74.
Van Heuvelen, K. M., Fiedler, A. T., Shan, X., De Hont, R. F., Meier, K. K., Bominaar, E. L., Munck, E. & Que, L. (2012). *Proc. Natl Acad. Sci.* **8**, 11933–11938.
Zhao, Y. & Truhlar, D. G. (2008). *Theor. Chem. Acc.* **120**, 215–241.

supporting information

Acta Cryst. (2017). C**73**, 620-624 [https://doi.org/10.1107/S2053229617010397]

Crystal structure and spectroscopic characterization of a cobalt(II) tetraaza-macrocycle: completing a series of first-row transition-metal complexes

Katherine M. Van Heuvelen, Isabell Lee, Katherine Arriola, Rilke Griffin, Christopher Ye and Michael K. Takase

Computing details

Data collection: *APEX3* (Bruker, 2017); cell refinement: *SAINT* (Bruker, 2013); data reduction: *SAINT* (Bruker, 2013); program(s) used to solve structure: *SHELXS2013* (Sheldrick, 2008); program(s) used to refine structure: *SHELXL2016* (Sheldrick, 2015); molecular graphics: *SHELXTL* (Sheldrick, 2008); software used to prepare material for publication: *SHELXTL* (Sheldrick, 2008).

Chlorido(1,4,8,11-tetramethyl-1,4,8,11-tetraazacyclotetradecane-κ^4N)cobalt(II) chloride dihydrate

Crystal data

$[CoCl(C_{14}H_{32}N_4)]Cl\cdot 2H_2O$
$M_r = 422.30$
Monoclinic, $P2_1/c$
$a = 8.2864$ (8) Å
$b = 17.0679$ (16) Å
$c = 13.9733$ (14) Å
$\beta = 90.735$ (4)°
$V = 1976.1$ (3) Å^3
$Z = 4$
$F(000) = 900$
$D_x = 1.419$ Mg m^{-3}
Mo $K\alpha$ radiation, $\lambda = 0.71073$ Å
Cell parameters from 9870 reflections
$\theta = 2.5$–35.8°
$\mu = 1.15$ mm^{-1}
$T = 100$ K
Block, purple
0.40 × 0.30 × 0.25 mm

Data collection

Bruker D8 VENTURE Kappa Duo PHOTON 100 CMOS diffractometer
Radiation source: IμS HB micro-focus sealed tube
Detector resolution: 10.24 pixels mm^{-1}
φ and ω scans
Absorption correction: multi-scan (SADABS; Bruker, 2013)
$T_{min} = 0.691$, $T_{max} = 0.747$
72258 measured reflections
9577 independent reflections
7769 reflections with $I > 2\sigma(I)$
$R_{int} = 0.043$
$\theta_{max} = 36.4°$, $\theta_{min} = 2.5°$
$h = -13\rightarrow13$
$k = -28\rightarrow28$
$l = -23\rightarrow23$

Refinement

Refinement on F^2
Least-squares matrix: full
$R[F^2 > 2\sigma(F^2)] = 0.032$
$wR(F^2) = 0.066$
$S = 1.04$
9577 reflections
224 parameters
4 restraints
Primary atom site location: structure-invariant direct methods
Secondary atom site location: difference Fourier map
Hydrogen site location: mixed

H atoms treated by a mixture of independent and constrained refinement
$w = 1/[\sigma^2(F_o^2) + (0.0244P)^2 + 0.7824P]$ where $P = (F_o^2 + 2F_c^2)/3$

$(\Delta/\sigma)_{max} = 0.001$
$\Delta\rho_{max} = 0.56$ e Å^{-3}
$\Delta\rho_{min} = -0.56$ e Å^{-3}

Special details

Geometry. All e.s.d.'s (except the e.s.d. in the dihedral angle between two l.s. planes) are estimated using the full covariance matrix. The cell e.s.d.'s are taken into account individually in the estimation of e.s.d.'s in distances, angles and torsion angles; correlations between e.s.d.'s in cell parameters are only used when they are defined by crystal symmetry. An approximate (isotropic) treatment of cell e.s.d.'s is used for estimating e.s.d.'s involving l.s. planes.

Refinement. Refinement of F^2 against ALL reflections. The weighted *R*-factor *wR* and goodness of fit *S* are based on F^2, conventional *R*-factors *R* are based on *F*, with *F* set to zero for negative F^2. The threshold expression of $F^2 > \sigma(F^2)$ is used only for calculating *R*-factors(gt) *etc*. and is not relevant to the choice of reflections for refinement. *R*-factors based on F^2 are statistically about twice as large as those based on *F*, and *R*- factors based on ALL data will be even larger.
Low-temperature diffraction data (φ and ω scans) were collected on a Bruker AXS D8 VENTURE *KAPPA* diffractometer coupled to a PHOTON 100 CMOS detector with Mo $K\alpha$ radiation (λ = 0.71073 Å) from an $I\mu$S micro-source for the structure of compound (1). The structure was solved by direct methods using *SHELXS* (Sheldrick, 1990) and refined against F^2 on all data by full-matrix least-squares with *SHELXL2014* (Sheldrick, 2008) using established refinement techniques (Müller, 2009). All non-H atoms were refined anisotropically.

Fractional atomic coordinates and isotropic or equivalent isotropic displacement parameters (Å²)

	x	*y*	*z*	U_{iso}*/U_{eq}
Cl1	0.51121 (3)	0.66061 (2)	0.60021 (2)	0.01723 (5)
Cl2	0.06423 (3)	0.86258 (2)	0.50039 (2)	0.01387 (4)
Co1	0.70186 (2)	0.62697 (2)	0.71424 (2)	0.00774 (3)
N1	0.92925 (9)	0.61319 (5)	0.64915 (6)	0.01016 (14)
C1	1.06802 (11)	0.64827 (6)	0.70353 (7)	0.01284 (16)
H1A	1.168131	0.638070	0.667682	0.015*
H1B	1.078240	0.621100	0.765913	0.015*
C2	1.05589 (11)	0.73585 (6)	0.72198 (7)	0.01317 (17)
H2A	1.031204	0.762659	0.660694	0.016*
H2B	1.162105	0.755086	0.745178	0.016*
C3	0.92830 (11)	0.75832 (6)	0.79439 (7)	0.01311 (17)
H3A	0.944496	0.726034	0.852584	0.016*
H3B	0.945020	0.813761	0.812835	0.016*
C11	0.92116 (12)	0.64801 (6)	0.55156 (7)	0.01463 (17)
H11A	0.892834	0.703609	0.556246	0.022*
H11B	0.838966	0.620606	0.513205	0.022*
H11C	1.026354	0.642729	0.520950	0.022*
N2	0.75794 (9)	0.74860 (5)	0.76028 (6)	0.01052 (14)
C4	0.64897 (12)	0.75884 (6)	0.84295 (7)	0.01296 (17)
H4A	0.537548	0.768126	0.819173	0.016*
H4B	0.683263	0.805357	0.880333	0.016*
C5	0.65108 (11)	0.68738 (6)	0.90727 (7)	0.01222 (16)
H5A	0.760621	0.680253	0.935032	0.015*
H5B	0.575100	0.695196	0.960533	0.015*
C12	0.72070 (13)	0.81142 (6)	0.69011 (8)	0.01583 (18)
H12A	0.608937	0.805911	0.667317	0.024*
H12B	0.793923	0.807228	0.635831	0.024*

H12C	0.734623	0.862643	0.720811	0.024*
N3	0.60402 (9)	0.61598 (5)	0.85200 (6)	0.00892 (13)
C6	0.65983 (11)	0.54640 (6)	0.90793 (7)	0.01222 (16)
H6A	0.610241	0.548372	0.971971	0.015*
H6B	0.778208	0.550192	0.917275	0.015*
C7	0.62092 (12)	0.46739 (6)	0.86275 (7)	0.01314 (17)
H7A	0.639592	0.425825	0.911057	0.016*
H7B	0.505031	0.466325	0.844684	0.016*
C8	0.72004 (12)	0.44890 (6)	0.77465 (7)	0.01401 (17)
H8A	0.835687	0.456146	0.790969	0.017*
H8B	0.703973	0.393054	0.757900	0.017*
C13	0.42510 (11)	0.61438 (6)	0.84195 (7)	0.01385 (17)
H13A	0.392948	0.570952	0.799971	0.021*
H13B	0.387433	0.663945	0.814205	0.021*
H13C	0.377045	0.607174	0.905065	0.021*
N4	0.68022 (10)	0.49764 (5)	0.68876 (6)	0.01139 (14)
C9	0.80575 (12)	0.48387 (6)	0.61544 (7)	0.01512 (18)
H9A	0.765011	0.501631	0.552162	0.018*
H9B	0.828800	0.427073	0.611178	0.018*
C10	0.95983 (12)	0.52758 (6)	0.64065 (7)	0.01353 (17)
H10A	1.004203	0.507481	0.702014	0.016*
H10B	1.040874	0.518220	0.590476	0.016*
C14	0.52429 (13)	0.47017 (6)	0.64767 (8)	0.01698 (19)
H14A	0.494482	0.502896	0.592598	0.025*
H14B	0.440415	0.473888	0.696270	0.025*
H14C	0.534960	0.415567	0.626997	0.025*
O2W	0.12364 (11)	1.01349 (5)	0.36822 (6)	0.02094 (16)
H2W2	0.0802 (19)	1.0482 (9)	0.3992 (11)	0.031*
H2W1	0.114 (2)	0.9743 (9)	0.4022 (11)	0.031*
O1W	0.26421 (10)	0.71355 (5)	0.42894 (6)	0.01797 (15)
H1W1	0.3258 (18)	0.7025 (9)	0.4779 (10)	0.027*
H1W2	0.2118 (18)	0.7541 (8)	0.4498 (11)	0.027*

Atomic displacement parameters (Å²)

	U^{11}	U^{22}	U^{33}	U^{12}	U^{13}	U^{23}
Cl1	0.01406 (10)	0.02120 (12)	0.01628 (11)	−0.00094 (8)	−0.00644 (8)	0.00522 (9)
Cl2	0.01321 (9)	0.01239 (10)	0.01603 (10)	−0.00032 (7)	0.00103 (7)	−0.00044 (8)
Co1	0.00643 (5)	0.00968 (6)	0.00711 (5)	0.00036 (4)	0.00040 (4)	0.00065 (4)
N1	0.0095 (3)	0.0107 (3)	0.0102 (3)	0.0001 (3)	0.0018 (3)	0.0013 (3)
C1	0.0078 (3)	0.0153 (4)	0.0154 (4)	−0.0008 (3)	0.0001 (3)	0.0024 (3)
C2	0.0099 (4)	0.0147 (4)	0.0149 (4)	−0.0036 (3)	−0.0002 (3)	0.0019 (3)
C3	0.0114 (4)	0.0140 (4)	0.0138 (4)	−0.0026 (3)	−0.0018 (3)	−0.0008 (3)
C11	0.0164 (4)	0.0170 (4)	0.0106 (4)	−0.0008 (3)	0.0033 (3)	0.0027 (3)
N2	0.0101 (3)	0.0100 (3)	0.0114 (3)	0.0007 (3)	−0.0003 (3)	0.0010 (3)
C4	0.0131 (4)	0.0113 (4)	0.0145 (4)	0.0018 (3)	0.0023 (3)	−0.0025 (3)
C5	0.0127 (4)	0.0139 (4)	0.0101 (4)	−0.0006 (3)	0.0017 (3)	−0.0022 (3)
C12	0.0186 (4)	0.0106 (4)	0.0182 (5)	0.0024 (3)	−0.0003 (4)	0.0041 (3)

N3	0.0072 (3)	0.0104 (3)	0.0092 (3)	0.0001 (2)	0.0004 (2)	0.0002 (3)
C6	0.0120 (4)	0.0146 (4)	0.0101 (4)	0.0003 (3)	−0.0003 (3)	0.0035 (3)
C7	0.0135 (4)	0.0125 (4)	0.0135 (4)	−0.0008 (3)	0.0019 (3)	0.0039 (3)
C8	0.0159 (4)	0.0110 (4)	0.0151 (4)	0.0016 (3)	0.0023 (3)	0.0027 (3)
C13	0.0075 (3)	0.0181 (5)	0.0159 (4)	0.0004 (3)	0.0010 (3)	0.0004 (3)
N4	0.0121 (3)	0.0110 (3)	0.0111 (3)	−0.0012 (3)	0.0011 (3)	−0.0005 (3)
C9	0.0186 (4)	0.0125 (4)	0.0144 (4)	−0.0015 (3)	0.0055 (3)	−0.0031 (3)
C10	0.0135 (4)	0.0114 (4)	0.0159 (4)	0.0022 (3)	0.0060 (3)	−0.0007 (3)
C14	0.0177 (4)	0.0166 (5)	0.0165 (4)	−0.0069 (4)	−0.0014 (4)	−0.0022 (4)
O2W	0.0299 (4)	0.0149 (4)	0.0182 (4)	0.0042 (3)	0.0049 (3)	0.0003 (3)
O1W	0.0172 (3)	0.0177 (4)	0.0189 (4)	0.0032 (3)	−0.0026 (3)	0.0005 (3)

Geometric parameters (Å, º)

Cl1—Co1	2.3022 (3)	C12—H12C	0.9800
Co1—N3	2.1066 (8)	N3—C13	1.4877 (12)
Co1—N1	2.1158 (8)	N3—C6	1.4920 (12)
Co1—N2	2.2208 (9)	C6—C7	1.5218 (14)
Co1—N4	2.2427 (9)	C6—H6A	0.9900
N1—C10	1.4880 (13)	C6—H6B	0.9900
N1—C11	1.4883 (13)	C7—C8	1.5217 (14)
N1—C1	1.4953 (13)	C7—H7A	0.9900
C1—C2	1.5204 (14)	C7—H7B	0.9900
C1—H1A	0.9900	C8—N4	1.4937 (13)
C1—H1B	0.9900	C8—H8A	0.9900
C2—C3	1.5218 (14)	C8—H8B	0.9900
C2—H2A	0.9900	C13—H13A	0.9800
C2—H2B	0.9900	C13—H13B	0.9800
C3—N2	1.4934 (12)	C13—H13C	0.9800
C3—H3A	0.9900	N4—C14	1.4832 (13)
C3—H3B	0.9900	N4—C9	1.4880 (12)
C11—H11A	0.9800	C9—C10	1.5164 (14)
C11—H11B	0.9800	C9—H9A	0.9900
C11—H11C	0.9800	C9—H9B	0.9900
N2—C12	1.4828 (13)	C10—H10A	0.9900
N2—C4	1.4856 (12)	C10—H10B	0.9900
C4—C5	1.5152 (14)	C14—H14A	0.9800
C4—H4A	0.9900	C14—H14B	0.9800
C4—H4B	0.9900	C14—H14C	0.9800
C5—N3	1.4919 (12)	O2W—H2W2	0.820 (13)
C5—H5A	0.9900	O2W—H2W1	0.825 (13)
C5—H5B	0.9900	O1W—H1W1	0.869 (13)
C12—H12A	0.9800	O1W—H1W2	0.869 (12)
C12—H12B	0.9800		

N3—Co1—N1	137.57 (3)	H12A—C12—H12B	109.5
N3—Co1—N2	84.26 (3)	N2—C12—H12C	109.5
N1—Co1—N2	92.53 (3)	H12A—C12—H12C	109.5

N3—Co1—N4	91.52 (3)	H12B—C12—H12C	109.5
N1—Co1—N4	83.81 (3)	C13—N3—C5	108.51 (7)
N2—Co1—N4	169.13 (3)	C13—N3—C6	109.67 (7)
N3—Co1—Cl1	112.70 (2)	C5—N3—C6	107.56 (7)
N1—Co1—Cl1	109.71 (2)	C13—N3—Co1	108.07 (6)
N2—Co1—Cl1	96.12 (2)	C5—N3—Co1	107.42 (5)
N4—Co1—Cl1	94.75 (2)	C6—N3—Co1	115.42 (6)
C10—N1—C11	108.94 (8)	N3—C6—C7	115.18 (8)
C10—N1—C1	107.64 (7)	N3—C6—H6A	108.5
C11—N1—C1	109.33 (7)	C7—C6—H6A	108.5
C10—N1—Co1	107.28 (5)	N3—C6—H6B	108.5
C11—N1—Co1	108.64 (6)	C7—C6—H6B	108.5
C1—N1—Co1	114.86 (6)	H6A—C6—H6B	107.5
N1—C1—C2	115.32 (8)	C8—C7—C6	113.94 (8)
N1—C1—H1A	108.4	C8—C7—H7A	108.8
C2—C1—H1A	108.4	C6—C7—H7A	108.8
N1—C1—H1B	108.4	C8—C7—H7B	108.8
C2—C1—H1B	108.4	C6—C7—H7B	108.8
H1A—C1—H1B	107.5	H7A—C7—H7B	107.7
C1—C2—C3	114.11 (8)	N4—C8—C7	114.74 (8)
C1—C2—H2A	108.7	N4—C8—H8A	108.6
C3—C2—H2A	108.7	C7—C8—H8A	108.6
C1—C2—H2B	108.7	N4—C8—H8B	108.6
C3—C2—H2B	108.7	C7—C8—H8B	108.6
H2A—C2—H2B	107.6	H8A—C8—H8B	107.6
N2—C3—C2	114.95 (8)	N3—C13—H13A	109.5
N2—C3—H3A	108.5	N3—C13—H13B	109.5
C2—C3—H3A	108.5	H13A—C13—H13B	109.5
N2—C3—H3B	108.5	N3—C13—H13C	109.5
C2—C3—H3B	108.5	H13A—C13—H13C	109.5
H3A—C3—H3B	107.5	H13B—C13—H13C	109.5
N1—C11—H11A	109.5	C14—N4—C9	107.26 (8)
N1—C11—H11B	109.5	C14—N4—C8	108.50 (8)
H11A—C11—H11B	109.5	C9—N4—C8	108.42 (8)
N1—C11—H11C	109.5	C14—N4—Co1	116.11 (6)
H11A—C11—H11C	109.5	C9—N4—Co1	102.10 (6)
H11B—C11—H11C	109.5	C8—N4—Co1	113.85 (6)
C12—N2—C4	107.79 (8)	N4—C9—C10	110.88 (8)
C12—N2—C3	108.57 (8)	N4—C9—H9A	109.5
C4—N2—C3	108.68 (8)	C10—C9—H9A	109.5
C12—N2—Co1	116.32 (6)	N4—C9—H9B	109.5
C4—N2—Co1	102.02 (6)	C10—C9—H9B	109.5
C3—N2—Co1	112.94 (6)	H9A—C9—H9B	108.1
N2—C4—C5	111.35 (8)	N1—C10—C9	110.97 (8)
N2—C4—H4A	109.4	N1—C10—H10A	109.4
C5—C4—H4A	109.4	C9—C10—H10A	109.4
N2—C4—H4B	109.4	N1—C10—H10B	109.4
C5—C4—H4B	109.4	C9—C10—H10B	109.4

H4A—C4—H4B	108.0	H10A—C10—H10B	108.0
N3—C5—C4	110.45 (8)	N4—C14—H14A	109.5
N3—C5—H5A	109.6	N4—C14—H14B	109.5
C4—C5—H5A	109.6	H14A—C14—H14B	109.5
N3—C5—H5B	109.6	N4—C14—H14C	109.5
C4—C5—H5B	109.6	H14A—C14—H14C	109.5
H5A—C5—H5B	108.1	H14B—C14—H14C	109.5
N2—C12—H12A	109.5	H2W2—O2W—H2W1	103.8 (16)
N2—C12—H12B	109.5	H1W1—O1W—H1W2	101.5 (14)
C10—N1—C1—C2	−178.34 (8)	C13—N3—C6—C7	61.68 (10)
C11—N1—C1—C2	63.46 (10)	C5—N3—C6—C7	179.50 (8)
Co1—N1—C1—C2	−58.94 (9)	Co1—N3—C6—C7	−60.63 (9)
N1—C1—C2—C3	70.73 (11)	N3—C6—C7—C8	71.35 (11)
C1—C2—C3—N2	−70.86 (11)	C6—C7—C8—N4	−69.80 (11)
C2—C3—N2—C12	−73.00 (10)	C7—C8—N4—C14	−74.47 (10)
C2—C3—N2—C4	170.00 (8)	C7—C8—N4—C9	169.34 (8)
C2—C3—N2—Co1	57.55 (9)	C7—C8—N4—Co1	56.47 (10)
C12—N2—C4—C5	166.95 (8)	C14—N4—C9—C10	166.18 (8)
C3—N2—C4—C5	−75.56 (10)	C8—N4—C9—C10	−76.84 (10)
Co1—N2—C4—C5	43.96 (8)	Co1—N4—C9—C10	43.64 (9)
N2—C4—C5—N3	−57.53 (10)	C11—N1—C10—C9	−79.54 (9)
C4—C5—N3—C13	−79.89 (9)	C1—N1—C10—C9	162.01 (8)
C4—C5—N3—C6	161.54 (7)	Co1—N1—C10—C9	37.89 (9)
C4—C5—N3—Co1	36.71 (8)	N4—C9—C10—N1	−58.26 (11)

Hydrogen-bond geometry (Å, º)

D—H···*A*	*D*—H	H···*A*	*D*···*A*	*D*—H···*A*
C2—H2*A*···Cl2^{i}	0.99	2.83	3.7784 (11)	160
C3—H3*A*···Cl2^{ii}	0.99	2.74	3.7054 (11)	166
C11—H11*C*···O1*W*^{i}	0.98	2.66	3.5203 (13)	147
C5—H5*A*···Cl2^{ii}	0.99	2.76	3.7452 (10)	171
C12—H12*A*···Cl1	0.98	2.77	3.3409 (11)	118
C7—H7*A*···Cl2^{iii}	0.99	2.94	3.6790 (10)	132
C8—H8*A*···O2*W*^{ii}	0.99	2.66	3.6324 (14)	168
C13—H13*C*···Cl2^{iv}	0.98	2.97	3.7640 (10)	138
C9—H9*B*···O1*W*^{v}	0.99	2.58	3.4736 (13)	150
C10—H10*A*···O2*W*^{ii}	0.99	2.54	3.5121 (14)	168
C14—H14*A*···Cl1	0.98	2.70	3.3189 (12)	122
O2*W*—H2*W*2···Cl2^{vi}	0.82 (1)	2.40 (1)	3.2158 (9)	173 (2)
O2*W*—H2*W*1···Cl2	0.83 (1)	2.39 (1)	3.2110 (9)	175 (2)
O1*W*—H1*W*1···Cl1	0.87 (1)	2.39 (1)	3.2568 (9)	173 (1)
O1*W*—H1*W*2···Cl2	0.87 (1)	2.33 (1)	3.2024 (9)	178 (1)

Symmetry codes: (i) *x*+1, *y*, *z*; (ii) *x*+1, −*y*+3/2, *z*+1/2; (iii) −*x*+1, *y*−1/2, −*z*+3/2; (iv) *x*, −*y*+3/2, *z*+1/2; (v) −*x*+1, −*y*+1, −*z*+1; (vi) −*x*, −*y*+2, −*z*+1.